Chemical Papers (2023) 77:2317–2325
https://doi.org/10.1007/s11696-022-02618-x

SHORT COMMUNICATION

A highly selective fluorescent probe for the detection of exogenous and endogenous hypochlorous acid/hypochlorite

Huiqin Wei[1] · Meixia Tan[2] · Yitong Lin[2] · Houzheng Chen[2] · Xinyao Wu[2] · Zhiqiang Zhang[2] · Fang Ke[2]

Received: 14 September 2022 / Accepted: 2 December 2022 / Published online: 9 December 2022
© Institute of Chemistry, Slovak Academy of Sciences 2022

Abstract

Hypochlorous acid/hypochlorite ($HOCl/OCl^-$) plays a crucial role in immune defense and other biological processes. A carbazole fluorescent probe, 9-ethyl-3-((2-(4-nitrophenyl)hydrazineylidene) methyl)-9H-carbazole (CZ-NH), was designed and synthesized for the detection of $HOCl/OCl^-$. After OCl^- was added, the fluorescence spectrum showed a strong absorption peak at 370 nm, and the fluorescence enhancement was nearly 500 times. The probe has strong selectivity for OCl^-, low detection limit 2.709 μM, non-toxicity to cells, good permeability and can be used for fluorescence imaging of exogenous and endogenous OCl^-, indicating that CZ-NH has potential biological application value. The probe CZ-NH was characterized by ^{1}H NMR and ^{13}C NMR. In addition, the recognition mechanism of OCl^- was verified by mass spectrometry and density functional theory (DFT).

Graphical abstract

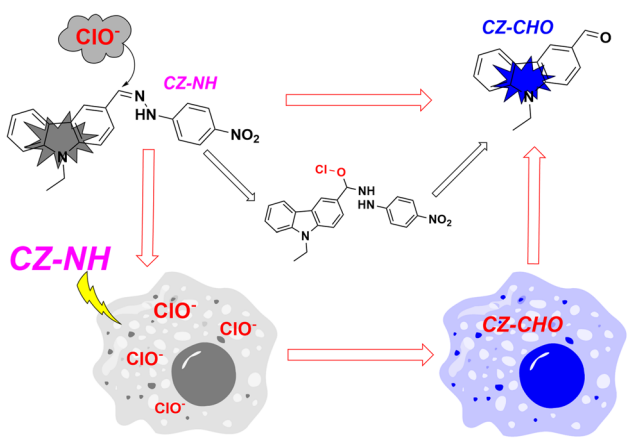

Keywords Hypochlorous acid · Carbazole · Fluorescence imaging

✉ Huiqin Wei
1412018003@qq.com

✉ Zhiqiang Zhang
zzq@fjmu.edu.cn

✉ Fang Ke
kefang@mail.fjmu.edu.cn

[1] Fujian Medical University Union Hospital, Interventional Catheter Room, Fuzhou 350001, China

[2] School of Pharmacy, Institute of Materia Medica, Fujian Provincial Key Laboratory of Natural Medicine Pharmacology, Fujian Medical University, Fuzhou 350004, China

Introduction

$HOCl/OCl^-$ is one of the most important reactive oxygen species (ROS). It is produced by the reaction of chloride ions and hydrogen peroxide catalyzed by myeloperoxidase (MPO) in living organisms and is involved in many physiological and pathological processes in the body (Harrison and Schultz 1976; Kettleet and Winterbourn 1997; Sivaraman et al. 2014; Raja et al. 2017; Ponnuvel et al. 2018; Perumal et al. 2020; Swamy et al. 2020). The change of

HOCl concentration is closely related to the functional state of cells. At physiological concentrations, HOCl provides a guarantee for human body to resist pathogen and bacterial invasion through its strong oxidation and bactericidal ability (Chen et al. 2011) However, once the concentration of HOCl is abnormal, it will directly damage organelles and tissues in the body, thus leading to the occurrence of disease. It has been reported that the concentration of ROS in cancer cells is about 10 times higher than that in normal cells (Wang et al. 2021; Antunes and Cadenas 2001; Wang et al. 2022), which may help distinguish cancer cells from normal cells. Therefore, it is still of great significance to track the real-time detection of HOCl in the body.

In recent decades, there have been numerous reports on the detection of HOCl/OCl^-, such as mass spectrometry (Peris-Díaz et al. 2021), electroanalysis (Wang et al. 2008), and chemiluminescence. In recent decades, there have been numerous reports on the detection of HOCl/OCl^-, such as potentiometric, electroanalytical, and chemiluminescence methods. However, due to the high cost and complicated operation of these methods, more attention has been paid to the effective detection of HOCl by fluorescent probes. The HOCl fluorescent probe design strategy is based on the reaction between HOCl and specific functional groups. At present, the main types reported are oxidation deoxime mechanism (Nguyena et al. 2018), oxidation of sulfur-containing elements (S, Se, Te elements) atom or group mechanism (Kenmoku et al. 2007; Koide et al. 2011; Wu et al. 2017; Yuan et al. 2015; Xu et al. 2015), oxidation of *p*-methyl phenol or *p*-methoxyaniline mechanism (Zhou et al. 2012; Sun et al. 2008; Hu et al. 2016, 2014), desulfurization cyclization (Hua et al. 2019), oxidation of carbon–carbon double bond (Zou et al. 2019; Chen et al. 2010), oxidation of deiminomaleonitrile (Zhu et al. 2014; He et al. 2020), etc. (Table 1).

In recent years, fluorescent probes have been favored by chemical biologists due to their excellent characteristics such as high sensitivity, good selectivity, short response time, low cost, easy operation, and in situ imaging (Zhu et al. 2018; Chen et al. 2016; Xu et al. 2016). In addition, fluorescent probes can enter a single cell for accurate detection and can realize the detection of active substances or metabolites in organisms, which is of great significance for the development of modern biology. It is well known that outstanding photostability, biological compaction, solubility, reliable molar absorption coefficient, and fluorescence quantum yield are all requisites in the application of developed fluorophores (Dwight and Levin 2016). For this reason, through the continuous attempts and innovations of many researchers, many fluorescent probes have been invented based on 2-(2-hydroxyphenyl) benzothiazole (Zhu et al. 2021a, b), BODIPY (Venkatesan and Wu 2015; Liu et al. 2016; Liu and Wu 2013), coumarin (Duan et al. 2019), fluorescein (Ren et al. 2022), naphthalimide (Feng et al. 2016), naphthalene (Zhang et al. 2020), rhodamine (Xiong et al. 2016; Mao et al. 2019; Yuichiro et al. 2011), 7-nitrobenz-2-oxa-1,3-diazole (NBD) (Jiao et al. 2020), etc. Therefore, it is urgent to synthesize fluorescent probes with simplicity, high sensitivity, good selectivity, low detection limit, and good photostability.

In this paper, a small molecule fluorescent probe, 9-ethyl-3-((2-(4-nitrophenyl) hydrazineylidene)methyl)-9H-carbazole (CZ-NH) with high selectivity for HOCl, was designed by using carbon–nitrogen double bond as the recognition functional group and carbazole with large conjugate system as the fluorophore. CZ-NH showed good quantum yield ($\Phi = 0.14$). When CZ-NH reacts with HOCl, CZ-CHO with strong fluorescence is released, which enhances the fluorescence and achieves the purpose of detection.

Experimental

Materials and chemicals

All other chemicals used in this article were obtained from commercial suppliers and can be used without further purification. The water is deionized. Silica gel for column chromatography was obtained from 200–300 mesh Sinopharm Chemical Reagent Co., LTD.. DMSO-d_6 was used as the solvent to record ^{1}H NMR spectrum at 400 MHz and 101 MHz (Bruker DPX) at ^{13}C NMR spectrum. Chemical shifts were reported in ppm with TMS as internal standard. Mass spectra were determined by high-resolution mass spectrometer. Absorption spectra were recorded on a Shimadzu UV-2600 spectrophotometer, and fluorescence spectra were recorded on a Cary Eclipse fluorometer. Cell imaging was recorded on a Leica inverted microscope.

Synthesis of compound CZ-NH

Synthesis of 9-ethyl-9H-carbazole-3-carbaldehyde (CZ-CHO): The solution of DMF (0.13 mL) and 1,2-dichloroethane (3 mL) was put into a round-bottom flask at 0 °C, $POCl_3$ was slowly dropped into the mixture, and then, *N*-ethyl carbazole dissolved in 1,2-dichloroethane was added to the mixture by drop (Scheme 1). The mixture was heated and stirred at 90 °C for 12 h, and the reaction solution was slowly poured into ice water after the reaction was complete. The products were extracted by ethyl acetate, dried and purified by column chromatography.^{1}H NMR (400 MHz, DMSO-d_6) δ 10.06 (s, 1H), 8.74 (d, $J = 1.6$ Hz, 1H), 8.28 (d, $J = 7.8$ Hz, 1H), 7.99 (dd, $J = 8.6$, 1.6 Hz, 1H), 7.74 (d, $J = 8.5$ Hz, 1H), 7.67 (d, $J = 8.3$ Hz, 1H), 7.53 (ddd, $J = 8.2$, 7.1, 1.2 Hz, 1H), 7.30 (t, $J = 7.5$ Hz, 1H), 4.47 (q, $J = 7.1$ Hz, 2H), 1.31 (t,

Table 1 Comparisons of this method and other different mechanism for detecting hypochlorous acid/hypochlorite

Fluorescence probe	Machanism	Wavelengths/nm	Limit of dection	Response time
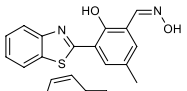	oxidation deoxime mechanism	350/540	80 nM	15 min
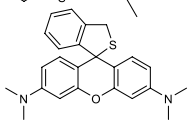	oxidation of sulfur-containing elements (S, Se, Te elements) atom or group mechanism	552/575	-	-
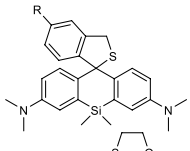	oxidation of sulfur-containing elements (S, Se, Te elements) atom or group mechanism	652/670	-	4 min
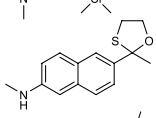	oxidation of sulfur-containing elements (S, Se, Te elements) atom or group mechanism	-/500	16.6 nM	within seconds
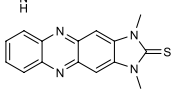	oxidation of sulfur-containing elements (S, Se, Te elements) atom or group mechanism	378/420,505	71 nM	30 min
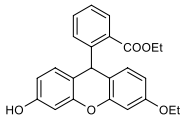	oxidation of p-methyl phenol or p-methoxylaniline mechanism	415/485	6.68 nM	20 min
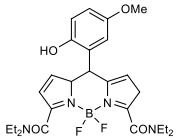	oxidation of p-methyl phenol or p-methoxylaniline mechanism	520/541	-	-
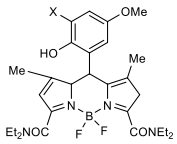	oxidation of p-methyl phenol or p-methoxylaniline mechanism	525/550	37 nM	within 15 min
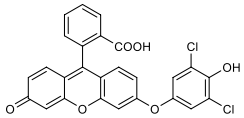	oxidation of p-methyl phenol or p-methoxylaniline mechanism	455/527	0.33 nM	within 1 min
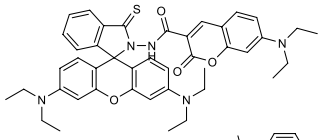	desulfurization cyclization	420/480,590	140 nM	1.5 min
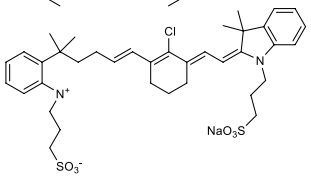	oxidation of carbon-carbon double bond	730/808,980	3.6 nM	-
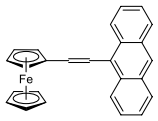	oxidation of carbon-carbon double bond	360/441	0.3 μM	10 min
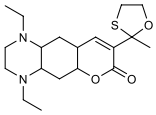	oxidation of deiminomaleonitrile	583/650	2.7 nM	within seconds
This work	oxidation of carbon-nitrogen oxide double bond	300/370	2.709 μM	20 min

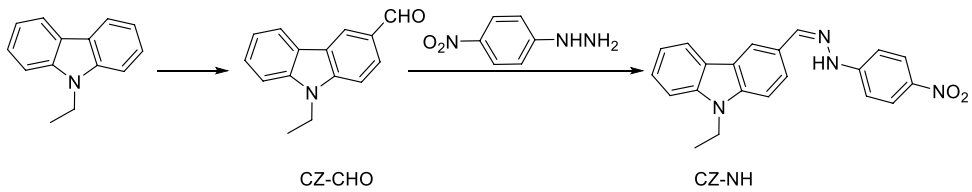

Scheme 1 Design and synthesis of the CZ-NH

$J = 7.2$ Hz, 3H). ^{13}C NMR (101 MHz, DMSO-d_6) δ 192.31, 143.50, 140.79, 128.71, 127.20, 127.10, 124.49, 122.82, 122.77, 121.33, 120.57, 110.31, 110.00, 37.80, 14.15.

Synthesis of CZ-NH (Zhu et al. 2021a, b): Add CZ-CHO (1 mmol) and *p*-nitrophenylhydrazine (1.5 mmol) to a round-bottomed flask, dissolve with absolute ethanol, and heat under reflux at 80 °C for 6 h. After the reaction, the excess solvent was removed, and the product was recrystallized from anhydrous ethanol.^{1}H NMR (400 MHz, DMSO-d_6) δ 11.26 (s, 1H), 8.48 (s, 1H), 8.25 (d, $J = 5.7$ Hz, 2H), 8.15 (d, $J = 9.1$ Hz, 2H), 7.93 (d, $J = 8.5$ Hz, 1H), 7.65 (dd, $J = 13.7$, 8.4 Hz, 2H), 7.49 (t, $J = 7.7$ Hz, 1H), 7.27–7.16 (m, 3H), 4.46 (q, $J = 7.1$ Hz, 2H), 1.33 (t, $J = 7.1$ Hz, 3H). ^{13}C NMR (101 MHz, DMSO-d_6) δ 151.34, 143.95, 140.70, 140.45, 138.24, 126.73, 126.61, 126.20, 124.59, 122.88, 122.63, 121.12, 120.08, 119.73, 111.47, 110.03, 109.91, 37.61, 14.24.

Fluorescence experiments

Prepare NaClO stock solutions (1 mM) and other analytes in deionized water. Probe 1 (1 mM) stock solution was prepared in DMSO. Various analyte stock solutions and probe stock solutions were taken into test tubes, and a mixture of DMSO and deionized water (1:1, *v/v*) containing phosphate-buffered saline (PBS, 20 mM, pH 7.4) was used. Dilute to desired concentration. All measurements were performed at room temperature (25 °C). All spectra were acquired in quartz cuvettes (200 μL). The excitation wavelength was 300 nm, and the excitation and emission slit widths were both 5 nm.

Cell culture and imaging

The cells were placed in Dulbecco's modified Eagle's medium (DMEM) supplemented with 10% fetal bovine serum (FBS), streptomycin (80 mg/L), and penicillin (80 units/mL), incubated in a humidified CO_2 incubator (37 °C) for 24 h. The cytotoxic effect of CZ-NH on RAW 264.7 cells was determined by standard methylthiazol tetrazolium (MTT) method.

The control group was treated with CZ-NH (10 μM) and washed with PBS buffer for three times. The exogenous and endogenous NaClO groups were pretreated with NaClO (500 μM) or lipopolysaccharide (LPS, 1 mM). The cells were incubated with CZ-NH (10 μM) for 30 min and washed with PBS for three times. Finally, live cells were imaged using a fluorescent inverted microscope.

Results and discussion

The probe mother liquor is composed of DMSO. The fluorescence intensity of the probe solution without NaClO at 370 nm is very weak, while the fluorescence intensity at 370 nm is significantly enhanced after NaClO is added. The results show that NaClO can increase the fluorescence intensity of the probe, because NaClO can oxidatively destroy C=N, while the *p*-NO_2 group is a strong electron-withdrawing group, which makes C=N more unstable. The presence of free CZ-CHO in solution resulted in enhanced fluorescence. It indicates that the CZ-NH can detect OCl^- sensitively.

Reaction time is an important indicator to measure whether a probe can be used for monitoring and analysis, so we first studied the specific situation of the reaction time between probe and NaClO. As shown in Fig. 1a, after NaClO was added to the probe buffer solution, the fluorescence intensity of the probe first strengthened with the prolongation of time. When the reaction time reached 20 min, the fluorescence intensity of the probe tended to be stable. The results show that the probe can be used as an effective method for rapid detection of NaClO.

The response of probe to NaClO at different pH is an important factor to determine whether probe can play an effective role. As shown in Fig. 1b, after adding buffer solutions of different pH to the mixture of probe and NaClO, the fluorescence intensity did not change with the change of pH, but tended to a stable state. When pH is 7.4, the fluorescence intensity reached the maximum value. It shows that the probe is suitable for the detection of NaClO in human body.

We also explored the selectivity of the probes for different analytes (including Cu^{2+}, Ni^{2+}, Zn^{2+}, Fe^{3+}, K^+, Ca^{2+}, Al^{3+}, Na^+, Cys, Hcy, His, Arg, Lys, NO_3^-, NO_2^-, Br^-, $H_2PO_4^-$, CH_3COO^-, ·OH, $O_2\cdot^-$, $ONOO^-$, H_2O_2, $^1O_2$, MnO_4^-, ClO_2^-, $Cr_2O_7^{2-}$), and the fluorescence intensity was significantly enhanced after the addition of NaClO, while the fluorescence intensity did not change significantly when others were added. As shown in Fig. 2, at the wavelength of

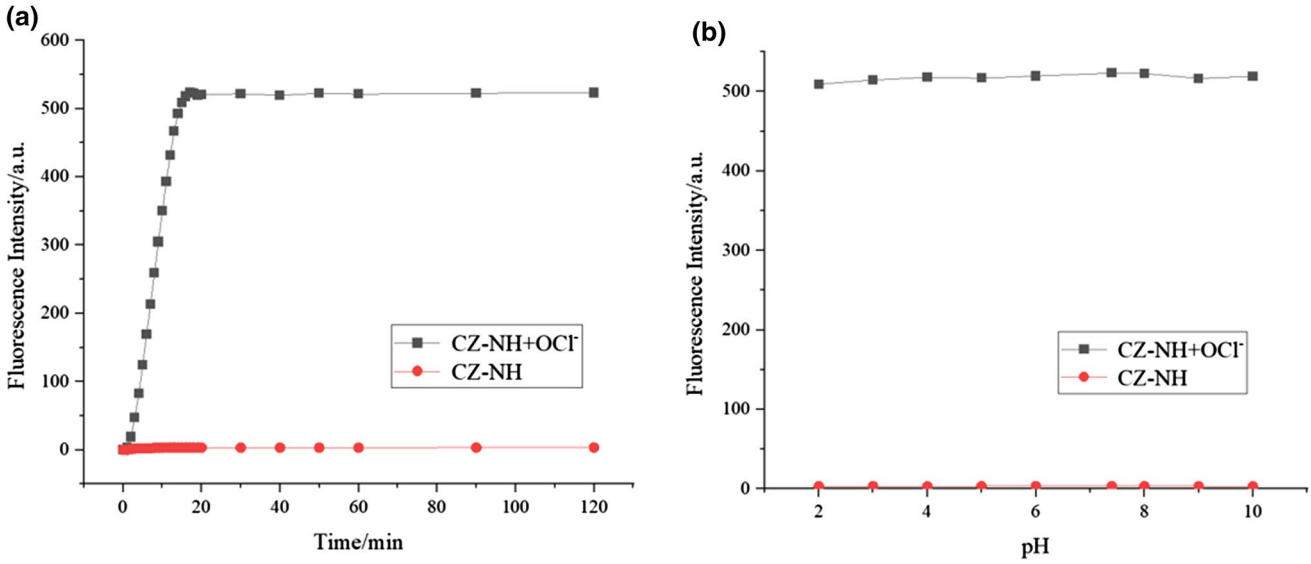

Fig. 1 **a** Effects of time on CZ-NH (10 μM) and its recognition ability for OCl^- in the aqueous solution of PBS (10 mM); **b** Effects of pH on CZ-NH (10 μM) and its recognition ability for OCl^- in the aqueous solution of PBS (10 mM). Excitation wavelength was 300 nm, and excitation and emission slit widths were 5 nm. The data represent the fluorescence intensities at 370 nm

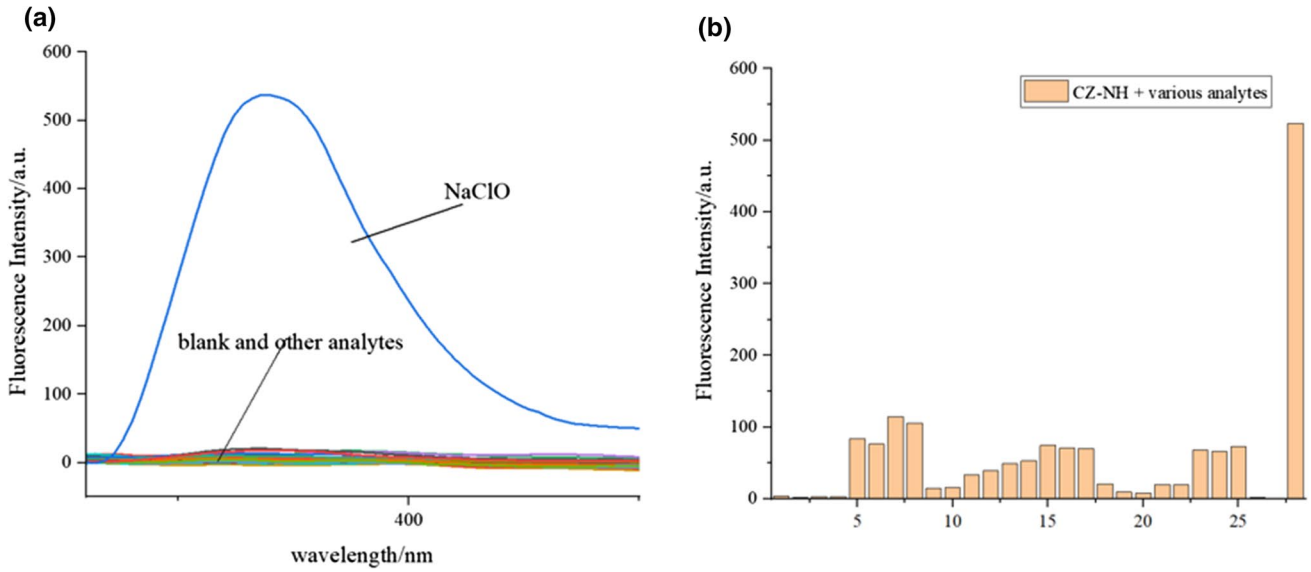

Fig. 2 **a** Fluorescence intensity of CZ-NH (10 μM) at 370 nm after addition of 10 mM selected ions; **b** Response values of probe CZ-NH and various analytes (1: Cu^{2+}, 2: Ni^{2+}, 3: Zn^{2+}, 4: Fe^{3+}, 5: K^+, 6: Ca^{2+}, 7: Al^{3+}, 8: Na^+, 9: Cys, 10: Hcy, 11: His, 12: Arg, 13: Lys, 14: NO_3^-, 15: NO_2^-, 16: Br^-, 17: $H_2PO_4^-$, 18: CH_3COO^-, 19: ·OH, 20: $O_2\cdot^-$, 21: $ONOO^-$, 22: H_2O_2, 23: $^1O_2$, 24: MnO_4^-, 25: ClO_2^-, 26: $Cr_2O_7^{2-}$,27: PBS, 28: $OCl.^-$)

370 nm, the fluorescence intensity generated by the addition of NaClO to CZ-NH was significantly enhanced, and the fluorescence intensity increased nearly 500-fold. The results showed that the selectivity of the probe to NaClO was better than that of other components (Table S1).

When the NaClO concentration ranged from 0 to 160 μM, the increase in fluorescence intensity showed a good linear relationship (Fig. 3b). The detection limit of this method is 2.709 μM, and it has good sensitivity for NaClO.

It is known that the conversion of *p*-nitrophenylhydrazone to aldehyde can be carried out by an oxidizing agent (McMucrry 1968). And hypochlorite has a strong oxidizing property, so the addition of OCl^- breaks the C=N in the probe structure, the reactive *p*-nitrophenylhydrazine group is

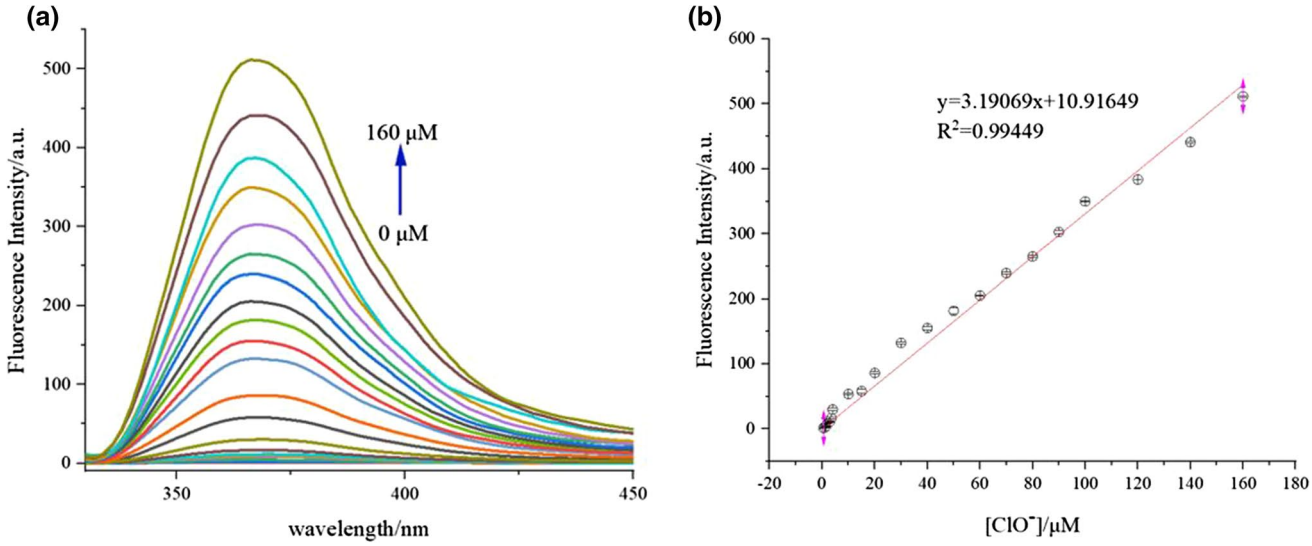

Fig. 3 **a** Fluorescence responses of CZ-NH (10 μM) to different concentrations of OCl^- in DMSO-PBS buffer (10 mM, pH 7.4) (*V*/*V* = 1:1); **b** The linear relationship between the fluorescence intensity and the concentration of NaClO. Excitation wavelength was 300 nm, and excitation and emission slit widths were 5 nm. The data represent the fluorescence intensities at 370 nm

cleaved and the free fluorophore CZ-CHO is released, resulting in significant fluorescence changes. To further understand the reaction mechanism between CZ-NH and OCl^-, the ESI–MS spectrum of CZ-NH in CH_3OH treated with OCl^- is shown in Supporting Information Fig. 3S. There is a peak at *m*/*z* = 224.09, corresponding to $[B+H]^+$ (Cal. 224.10), and *m*/*z* = 246.10, corresponding to $[B+Na]^+$ (Cal. 246.10). According to previous research results, the mechanism by which CZ-NH might recognize OCl^- is proposed, as shown in Scheme 2.

To further verify the proposed inter-probe mechanism, density functional theory (DFT) calculations were performed. Figure 4 lists the highest and lowest occupied molecular orbitals (HOMOs) for CZ-NH and CZ-CHO. The HOMO of CZ-CHO is mainly distributed on CZ-CHO, and the LUMO is all over the molecule. The large HOMO–LUMO gap (2.75 and 4.07 eV for CZ-NH and CZ-CHO HOMO–LUMO gaps, respectively) shows high stability of CZ-CHO upon addition of OCl^- converting CZ-NH to CZ-CHO. The results verify the reaction mechanism, and CZ-NH is highly selective and sensitive to OCl^-, which can enhance the fluorescence.

MTT assay was used to evaluate the cytotoxicity of RAW 264.7 cells. The results showed that the cell viability was more than 90% when the probe concentration was below 20.0 μM (Supporting Information Fig. 1S), indicating that CZ-NH had low cytotoxicity. Cells were pretreated with NaClO and LPS for 30 min at 37 °C and then incubated with CZ-NH (10 μM) for another 30 min at 37 °C. A strong blue fluorescence signal appeared in the cytoplasm

Scheme 2 Proposed response mechanism of CZ-NH to OCl^-

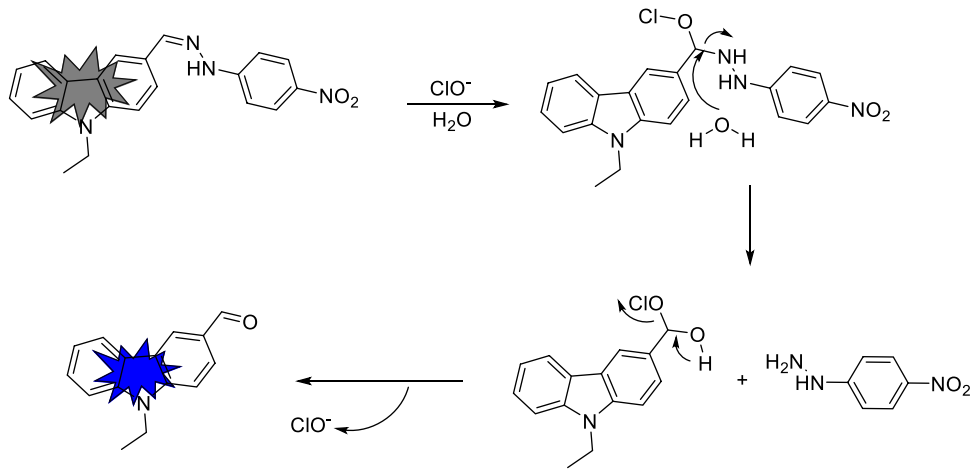

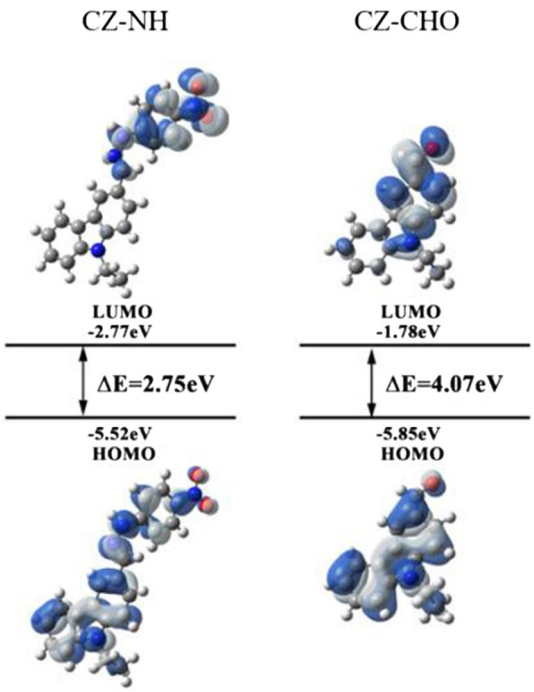

Fig. 4 Structure optimization diagram of probe CZ-NH and adding OCl^-

of the cells (Fig. 5), and the fluorescence of NaClO experimental group was significantly stronger than that of LPS experimental group. When treated with CZ-NH only for 30 min at 37 °C, there was almost no fluorescence signal in the cells (Fig. 5f). These results indicate that CZ-NH can detect NaClO in living cells.

Conclusions

We have successfully designed a novel carbazolyl fluorescent probe, CZ-NH, which can selectively react with NaClO. The addition of OCl^- broke the C=N in the probe structure, and the nitro group was a strong electron-withdrawing group, which accelerated the C=N cleavage and released the free fluorophore CZ-CHO, thus producing significant fluorescence changes and realizing its fluorescence detection. The addition of OCl^- increased the fluorescence intensity nearly 500 times, low detection limit 2.709 μM, and the probe CZ-NH had low toxicity, good biocompatibility, and could penetrate the cell membrane for intracellular imaging. The good permeability and staining ability further demonstrated the feasibility of CZ-NH to accurately monitor NaClO in biological systems.

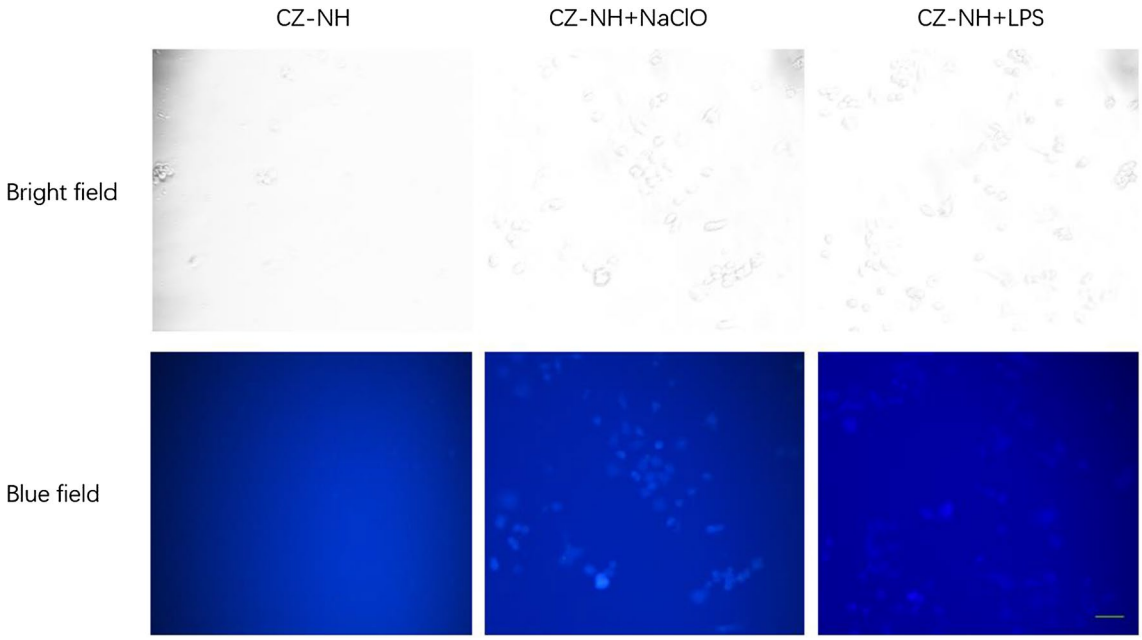

Fig. 5 Fluorescence imaging of RAW 264.7 cells. The first column shows cells treated with CZ-NH (10 μM) (**a** bright field; **d** blue channel); The second column shows cells treated with NaClO (500 μM) and CZ-NH (10 μM) (**b** bright field; **e** blue channel). The third column shows cells treated with LPS (LPS, 1 mM) and CZ-NH (10 μM) (**c** bright field; **f** blue channel). Scale bar: 10 μm

Supplementary Information The online version contains supplementary material available at https://doi.org/10.1007/s11696-022-02618-x.

Acknowledgements This work was supported by Fujian Provincial Natural Science Foundation (2020J01617) support.

Declarations

Conflicts of interest On behalf of all authors, the corresponding author states that there is no conflict of interest.

References

Antunes F, Cadenas E (2001) Cellular titration of apoptosis with steady-state concentrations of H_2O_2: submicromolar levels of H_2O_2 induce apoptosis through fenton chemistry independent of the cellular thiol state. Free Radic Biol Med 30(9):1008–1018. https://doi.org/10.1016/S0891-5849(01)00493-2

Chen SM, Lu JX, Sun CD, Ma HM (2010) A highly specific ferrocene-based fluorescent probe for hypochlorous acid and its application to cell imaging. Analyst 135(3):577–582. https://doi.org/10.1039/B921187J

Chen XQ, Wang F, Hyun JY, Wei TW, Qiang J, Ren XT, Shin I, Yoon J (2011) Fluorescent and luminescent probes for detection of reactive oxygen and nitrogen species. Chem Soc Rev 40(3):4783–4804. https://doi.org/10.1039/C1CS15037E

Chen X, Wang F, Hyun JY, Wei T, Qiang J, Ren X, Shin I, Yoon J (2016) Recent progress in the development of fluorescent, luminescent and colorimetric probes for detection of reactive oxygen and nitrogen species. Chem Soc Rev 45(10):2976–3016. https://doi.org/10.1039/C6CS00192K

Duan QX, Jia P, Zhuang ZH, Liu CY, Zhang X, Wang ZK, Sheng WL, Li ZL, Zhu HC, Zhu BC, Zhang XL (2019) Rational design of a hepatoma-specific fluorescent probe for HOCl and its bioimaging applications in living HepG2 cells. Anal Chem 91(3):2163–2168. https://doi.org/10.1021/acs.analchem.8b04726

Dwight SJ, Levin S (2016) Scalable regioselective synthesis of rhodamine dyes. Org Lett 18(20):5316–5319. https://doi.org/10.1021/acs.orglett.6b02635

Feng W, Qiao QL, Leng S, Miao L, Yin WT, Wang LQ, Xu ZC (2016) A 1,8-naphthalimide-derived turn-on fluorescent probe for imaging lysosomal nitric oxide in living cells. Chin Chem Lett 27(9):1554–1558. https://doi.org/10.1016/j.cclet.2016.06.016

Harrison JE, Schultz J (1976) Studies on the chlorinating activity of myeloperoxidase. J Biol Chem 251(5):1371–1374. https://doi.org/10.1016/S0021-9258(17)33749-3

He L, Xiong HQ, Wang BH, Zhang Y, Wang JP, Zhang HY, Li HP, Yang ZG, Song XZ (2020) Rational design of a two-photon ratiometric fluorescent probe for hypochlorous acid with a large stokes shift. Anal Chem 92(16):11029–11034. https://doi.org/10.1021/acs.analchem.0c00030

Hu JJ, Wong NK, Gu Q, Bai X, Ye S, Yang D (2014) HKOCl-2 series of green BODIPY based fluorescent probes for hypochlorous acid detection and imaging in live cells. Org Lett 16(13):3544–3547. https://doi.org/10.1021/ol501496n

Hu JJ, Wong NK, Lu MY, Chen X, Ye S, Zhao AQ, Gao P, Kao RYT, Shen J, Yang D (2016) HKOCl-3: a fluorescent hypochlorous acid probe for live-cell and in vivo imaging and quantitative application in flow cytometry and a 96-well microplate assay. Chem Sci 7(3):2094–2099. https://doi.org/10.1039/C5SC03855C

Hua JW, Zhang X, Liu TT, Gao HW, Lu SL, Uvdal K, Hu ZJ (2019) Ratiometric fluorogenic determination of endogenous hypochlorous acid in living cells. Spectrochim Acta A Mol Biomol Spectrosc 219(5):232–239. https://doi.org/10.1016/j.saa.2019.04.024

Jiao CP, Liu YY, Pang JX, Lu WJ, Zhang PP, Wang YF (2020) A simple lysosome-targeted probe for detection of hypochlorous acid in living cells. J Photochem Photobiol A 392:112399. https://doi.org/10.1016/j.jphotochem.2020.112399

Kenmoku S, Urano Y, Kojima H, Nagano T (2007) Development of a highly specific rhodamine-based fluorescence probe for hypochlorous acid and its application to real-time imaging of phagocytosis. J Am Chem Soc 129(23):7313–7318. https://doi.org/10.1021/ja068740g

Kettle AJ, Winterbourn CC (1997) Myeloperoxidase: a key regulator of neutrophil oxidant production. Redox Rep 3(1):3–15. https://doi.org/10.1080/13510002.1997.11747085

Koide Y, Urano Y, Hanaoka K, Terai T, Nagano T (2011) Development of an Sirhodamine-based far-red to near-infrared fluorescence probe selective for hypochlorous acid and its applications for biological imaging. J Am Chem Soc 133(15):5680–5682. https://doi.org/10.1021/ja111470n

Liu SR, Wu SP (2013) Hypochlorous acid turn-on fluorescent probe based on oxidation of diphenyl selenide. Org Lett 15(4):878–881. https://doi.org/10.1021/ol400011u

Liu Y, Zhao ZM, Miao JY, Zhao BX (2016) A ratiometric fluorescent probe based on boron dipyrromethene and rhodamine Förster resonance energy transfer platform for hypochlorous acid and its application in living cells. Anal Chim Acta 921:77–83. https://doi.org/10.1016/j.aca.2016.03.045

Mao GJ, Liang ZZ, Bi J, Zhang H, Meng HM, Su L, Gong YJ, Feng S, Zhang G (2019) A near-infrared fluorescent probe based on photostable Si-rhodamine for imaging hypochlorous acid during lysosome-involved inflammatory response. Anal Chim Acta 1048:143–153. https://doi.org/10.1016/j.aca.2018.10.014

McMurry JE (1968) Total synthesis of sativene. J Am Chem Soc 90(24):6821–6825. https://doi.org/10.1021/ja01026a046

Nguyena KH, Hao YQ, Zeng K, Fan SN, Li F, Yuan SK, Ding XJ, Xu MT, Liu YN (2018) A benzothiazole-based fluorescent probe for hypochlorous acid detection and imaging in living cells. Spectrochim Acta A Mol Biomol Spectrosc 199:189–193. https://doi.org/10.1016/j.saa.2018.03.055

Peris-Díaz MD, Guran R, Zitka O, Adam V, Krezel A, Guran R, Zitka O, Adam V, Krezel A (2021) Mass spectrometry-based structural analysis of cysteine-rich metal-binding sites in proteins with MetaOdysseus R software. J Proteome Res 20(1):776–785. https://doi.org/10.1021/acs.jproteome.0c00651

Perumal S, Karuppannan S, Gandhi S, Subramanian S, Govindasamy A, Gopal SK (2020) Bithiophene triarylborane dyad: an efficient material for the selective detection of CN^- and F^- ions. Appl Organomet Chem 34:e5257. https://doi.org/10.1002/aoc.5257

Ponnuvel K, Ramamoorthy J, Sivaraman G, Padmini V (2018) Merocyanine dye-based fluorescent chemosensor for highly selective and sensitive detection of hypochlorous acid and imaging in live cells. Chem Sel 3:91–95. https://doi.org/10.1002/slct.201701833

Raja SO, Sivaraman G, Mukherjee A, Duraisamy C, Gulyani A (2017) Facile synthesis of highly sensitive, red-emitting, fluorogenic dye for microviscosity and mitochondrial imaging in embryonic stem cells. Chem Sel 2(17):4609–4616. https://doi.org/10.1002/slct.201700463

Ren JY, Du ZB, Zhang WZ, Zhang R, Song B, Yuan JL (2022) Development of a fluorescein modified ruthenium (II) complex probe for lysosome-targeted ratiometric luminescence detection and imaging of peroxynitrite in living cells. Anal Chim Acta 1205:339784. https://doi.org/10.1016/j.aca.2022.339784

Sivaraman G, Anand T, Chellappa D (2014) A fluorescence switch for the detection of nitric oxide and histidine and its application in live cell imaging. ChemPlusChem 79(12):1761–1766. https://doi.org/10.1002/cplu.201402217

Sun ZN, Liu FQ, Chen Y, Tam PKH, Yang D (2008) A highly specific BODIPY-based fluorescent probe for the detection of hypochlorous acid. Org Lett 10(11):2171–2174. https://doi.org/10.1021/ol800507m

Swamy PCA, Sivaraman G, Priyanka RN, Raja SO, Ponnuvel K, Shanmugpriya J, Gulyani A (2020) Near infrared (NIR) absorbing dyes as promising photosensitizer for photo dynamic therapy. Coord Chem Rev 411:213233. https://doi.org/10.1016/j.ccr.2020.213233

Venkatesan P, Wu SP (2015) A turn-on fluorescent probe for hypochlorous acid based on the oxidation of diphenyl telluride. Analyst 140(4):1349–1355. https://doi.org/10.1039/C4AN02116A

Wang W, Li L, Liu SF, Ma CP, Zhang SH (2008) Determination of physiological thiols by electrochemical detection with piazselenole and its application in rat breast cancer cells 4T–1. J Am Chem Soc 130:10846–10847. https://doi.org/10.1021/ja802273p

Wang LF, Liu J, Zhang HX, Guo W (2021) Discrimination between cancerous and normal cells/tissues enabled by a near-infrared fluorescent HClO probe. Sens Actuat B-Chem 334:129602. https://doi.org/10.1016/j.snb.2021.129602

Wang K, Liu YL, Liu CY, Zhu HC, Li XW, Yu MH, Liu LY, Sang GQ, Sheng WL, Zhu BC (2022) A new-type HOCl-activatable fluorescent probe and its applications in water environment and biosystems. Sci Total Environ 839:156164. https://doi.org/10.1016/j.scitotenv.2022.156164

Wu L, Wu IC, DuFort CC, Carlson MA, Wu X, Chen L, Kuo CT, Qin Y, Yu J, Hingorani SR, Chiu DT (2017) Photostable ratiometric Pdot probe for in vitro and in vivo imaging of hypochlorous acid. J Am Chem Soc 139(20):6911–6918. https://doi.org/10.1021/jacs.7b01545

Xiong KM, Huo FJ, Yin CX, Chu YY, Yang YT, Chao JB, Zheng AM (2016) A novel recognition mechanism supported by experiment and theoretical calculation for hypochlorites recognition and its practical application. Sens Actuat B Chem 224:307–314. https://doi.org/10.1016/j.snb.2015.10.047

Xu Q, Heo CH, Kim G, Lee HW, Kim HM, Yoon J (2015) Development of imidazoline-2-thiones based two-photon fluorescence probes for imaging hypochlorite generation in a co-culture system. Angew Chem Int Ed 54(16):4890–4894. https://doi.org/10.1002/anie.201500537

Xu KH, Luan DR, Wang XT, Hu B, Liu XJ, Kong FP, Tang B (2016) An ultrasensitive cyclization-based fluorescent probe for imaging native HOBr in live cells and zebrafish. Angew Chem Int Ed 55(41):12751–12754. https://doi.org/10.1002/anie.201606285

Yuan L, Wang L, Agrawalla BK, Park SJ, Zhu H, Sivaraman B, Peng JJ, Xu QH, Chang YT (2015) Development of targetable two-photon fluorescent probes to image hypochlorous acid in mitochondria and lysosome in live cell and inflamed mouse model. J Am Chem Soc 137(18):5930–5938. https://doi.org/10.1021/jacs.5b00042

Yuichiro K, Yasuteru U, Kenjiro H, Takuya T, Tetsuo N (2011) Development of an Si-rhodamine-based far-red to near-infrared fluorescence probe selective for hypochlorous acid and its applications for biological imaging. J Am Chem Soc 133(15):5680–5682. https://doi.org/10.1021/ja111470n

Zhang WX, Jia Q, Meng YY, Chen SJ, Zhang YB, Wang KP, Gan LH, Hu ZQ (2020) Dimethylamino naphthalene-based fluorescent probes for hydrogen sulfide detection and living cell imaging. Spectrochim Acta A Mol Biomol Spectrosc 228:117835. https://doi.org/10.1016/j.saa.2019.117835

Zhou Y, Li JY, Chu KH, Liu K, Yao C, Li JY (2012) Fluorescence turn-on detection of hypochlorous acid via HOCl-promoted dihydrofluorescein-ether oxidation and its application in vivo. Chem Commun 48(39):4677–4679. https://doi.org/10.1039/C2CC30265A

Zhu H, Fan JL, Wang JY, Mu HY, Peng XJ (2014) An "enhanced PET"-based fluorescent probe with ultrasensitivityfor imaging basal and elesclomol-induced HClO in cancer cells. J Am Chem Soc 136(37):12820–12823. https://doi.org/10.1021/ja505988g

Zhu BC, Wang ZK, Zhao ZY, Shu W, Zhang M, Wu L, Liu CY, Duan QX, Jia P (2018) A simple highly selective and sensitive hydroquinone-based two-photon fluorescent probe for imaging peroxynitrite in live cells. Sens Actuat B Chem 262:380–385. https://doi.org/10.1016/j.snb.2018.01.203

Zhu JB, Li XM, Zhang SQ, Yan LQ (2021a) Synthesis and optical properties of Schiff base derivatives based on 2-(2-hydroxyphenyl) benzothiazole (HBT) and application in the detection of N_2H_4. Spectrochim Acta A Mol Biomol Spectrosc 257:119801. https://doi.org/10.1016/j.saa.2021.119801

Zhu TT, Hu Y, Chen X, Shao HB, Chen ZH, Zhang H, Liu CX (2021b) Novel chromene-derived fluorescent probe for detection of cyanides by imine-controlled ESIPT. Dye Pigments 195:109693. https://doi.org/10.1016/j.dyepig.2021.109693

Zou XM, Zhou XB, Cao C, Lu WY, Yuan W, Liu QY, Feng W, Li FY (2019) Dye-sensitized upconversion nanocomposites for ratiometric semi-quantitative detection of hypochlorite in vivo. Nanoscale 11(6):2959–2965. https://doi.org/10.1039/C8NR09531K

Publisher's Note Springer Nature remains neutral with regard to jurisdictional claims in published maps and institutional affiliations.